

Supporting Information

Design, synthesis and ring-opening polymerization of a new iodinated carbonate monomer: a universal route towards ultrahigh radiopaque aliphatic polycarbonates

Qian Ma, Kewen Lei, Jian Ding, Lin Yu*, Jiandong Ding

State Key Laboratory of Molecular Engineering of Polymers, Department of Macromolecular Science, Fudan University, Shanghai 200433, China, E-mail address:

yu_lin@fudan.edu.cn

Contents

Methods.....	3
High Resolution Mass Spectrometry (HRMS)	3
Gel Permeation Chromatography-Multi-angle Laser Light Scattering-Viscometer (GPC-MALS-VIS).....	3
X-ray Photoelectron Spectroscopy (XPS)	3
Thermo Gravimetric Analysis (TGA).....	4
Notes.....	4
Fig. S1.....	5
Fig. S2.....	6
Fig. S3.....	7
Fig. S4.....	8
Fig. S5.....	9
Fig. S6.....	10
Fig. S7.....	11
Fig. S8.....	12
Fig. S9.....	13
Fig. S10.....	14
Table S1.....	15
Table S2.....	16
Fig. S11.....	17
Fig. S12.....	18
Fig. S13.....	19
Fig. S14.....	20
Fig. S15.....	21
Fig. S16.....	22
Fig. S17.....	23
Fig. S18.....	24
Fig. S19.....	25
Fig. S20.....	26
Fig. S21.....	27
Fig. S22.....	28
Fig. S23.....	29
Notes and References.....	29

Methods

High Resolution Mass Spectrometry (HRMS). High-resolution mass spectrometry analysis was performed on a Bruker McriOTOF11 system scanning the 100–1500 m/z range with electrospray ionization (ESI) as ionization source. Some acquisition parameters were as follows: ion polarity: positive; dry gas flow rate: 6.0 L/mL; dry heater temperature: 200 °C; capillary voltage: 4000 V.

Gel Permeation Chromatography-Multi-angle Laser Light Scattering-Viscometer (GPC-MALS-VIS). The dn/dc result and absolute MW of the resultant polymers were measured on a 1260 Infinity GPC system (Agilent Technologies; Serial #: JPAAJ81960) coupled with a Wyatt refractive index detector (DAWN HELEOS-II, Model: WTREX-04; Serial #: 688-TREX) as well as a multi-angle light scattering (MALS) detector (Wyatt 6300 Hollister Ave, 658 nm, Model: WH2-06; Serial #: 1006-H2HC). THF was selected as the eluent at a flow rate of 1.0 mL/min at 35 °C and the sample injection volume was 100 μ L. The refractive index increment, dn/dc , was obtained via a Wyatt refractive index detector, which indicated the slope of the dependence of the refractive index (n) as a function of the polymer concentration (c). To guarantee sufficient light scattering signals for acquiring convincing results, the concentrations of polymers in THF were about 10 mg/mL for the GPC–MALS–VIS test. The final data were processed via ASTRA 6.1 software.

X-ray Photoelectron Spectroscopy (XPS). The XPS analysis was performed on a PHI 5000C ESCA System (US) equipped with a monochromatic Mg $K\alpha$ ($h\nu =$

1253.6 eV) X-ray source of 300 W at 14 kV. The binding energies of all recorded peaks in the XPS measurement were calibrated against 284.6 eV of the C1s peak. The final data was obtained using XPSPEAK4.1 software and processed furtherly by Origin software.

Thermo Gravimetric Analysis (TGA). Thermogravimetric measurements were performed on a Perkin Elmer Pyris 1 thermogravimetric analyzer at a heating rate of 10 °C/min under a flow of dry nitrogen (40 mL/min) and in the temperature range from 50 to 450 °C. The temperature of onset decomposition (T_d) is defined as the temperature when 5% weight loss occurs.

Notes: In ^1H NMR spectra, ITMC repeating unit is abbreviated as I; TMC repeating unit is abbreviated as T; GA repeating unit is abbreviated as G; *D,L*-LA repeating unit is abbreviated as L; ϵ -CL repeating unit is abbreviated as C; γ -VL repeating unit is abbreviated as V.

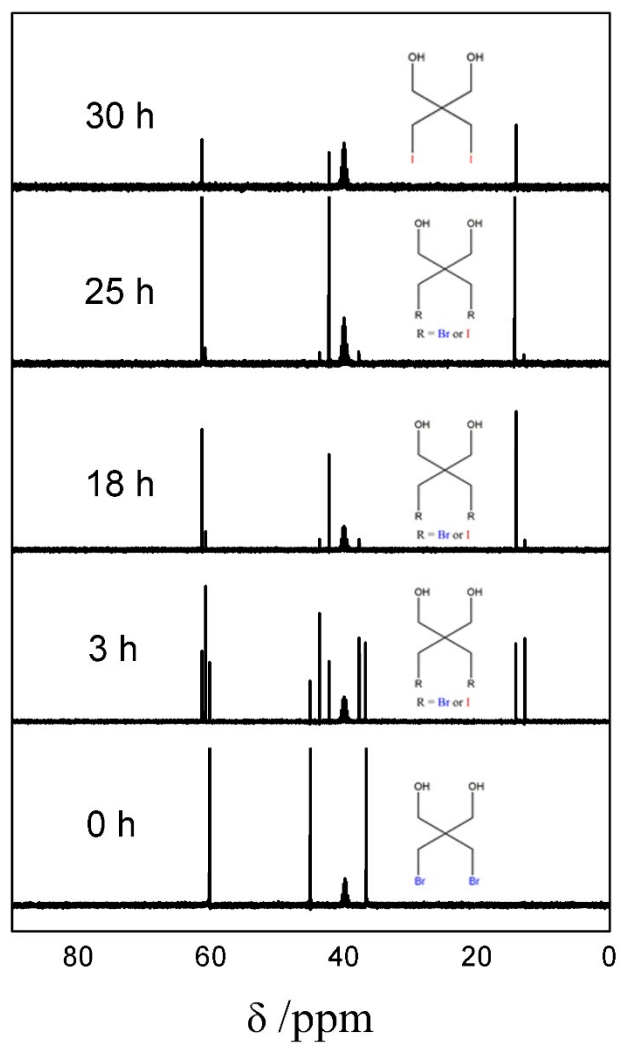


Fig. S1. ^{13}C NMR spectra of 2,2-bis(iodomethyl)propane-1,3-diol in the presence of excess sodium iodide as a function of reaction time.

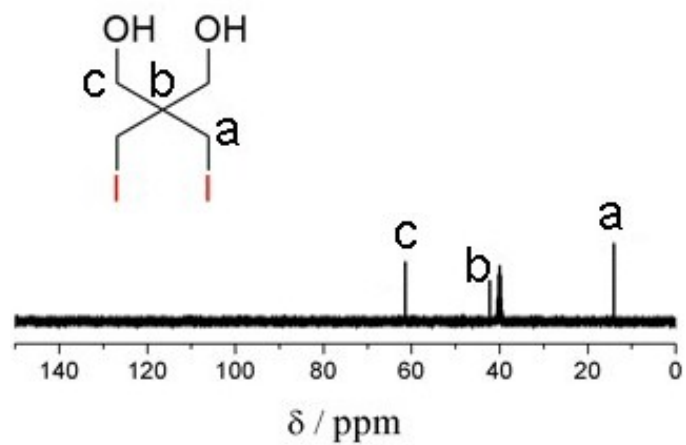
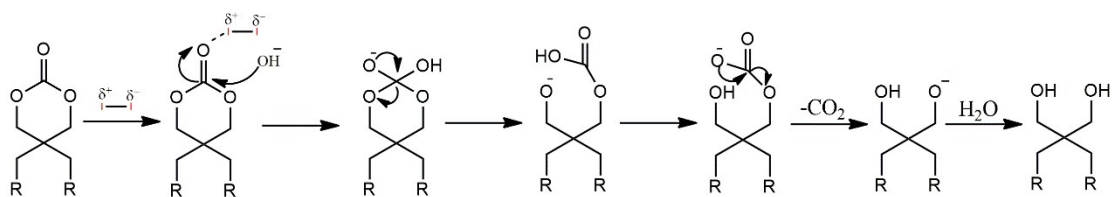
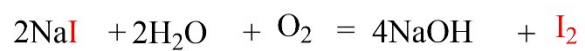


Fig. S2. ^{13}C NMR spectrum of the final product (Route 2) in $\text{DMSO-}d_6$.



R = Br or I

Fig. S3. The possible mechanism for structural damage of aliphatic carbonate monomer in Route 2.

As displayed in Fig. S4, all the characteristic peaks of monomers were well assigned. For example, the characteristic peak corresponding to the bromomethyl of the BTMC monomer was observed at 34 ppm, while the characteristic peak corresponding to the iodomethyl of the ITMC monomer appeared at 10 ppm.

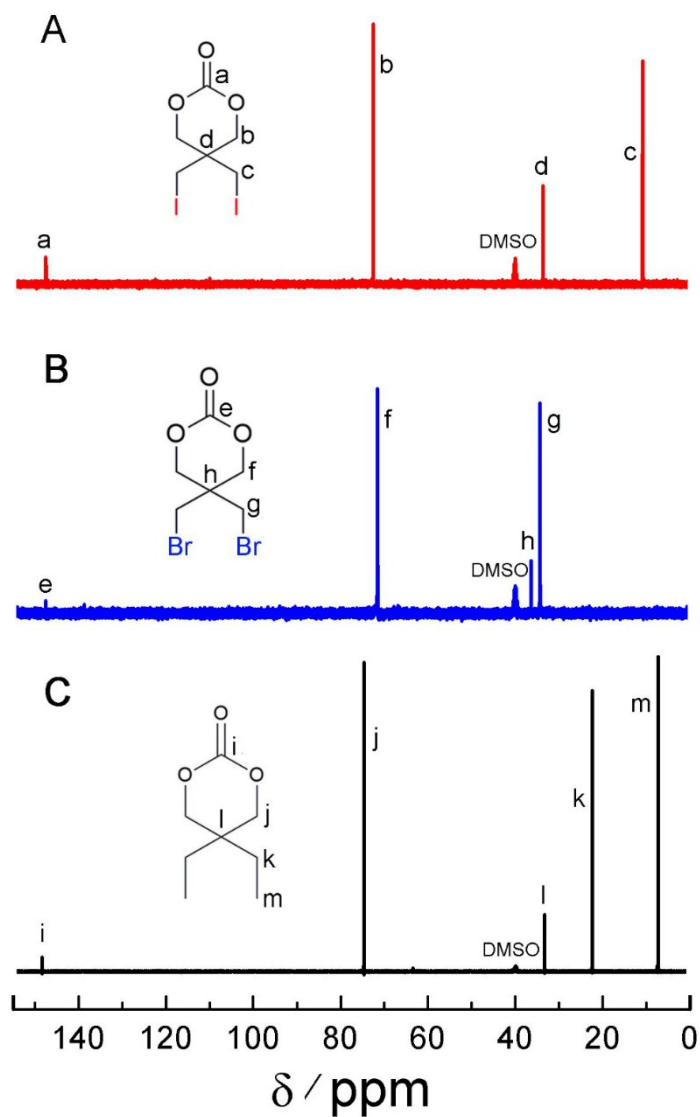


Fig. S4. ^{13}C NMR spectra of ITMC (A), BTMC (B) and ETMC (C) in $\text{DMSO}-d_6$.

In HRMS (Fig. S5), the presence of $m/z = 382.9$, 288.9 and 159.1 is attributed to the molecular ion (M^+) of ITMC monomer, BTMC monomer and ETMC monomer, respectively, which provided a direct evidence of the successful synthesis of desired functionalized TMC monomer.

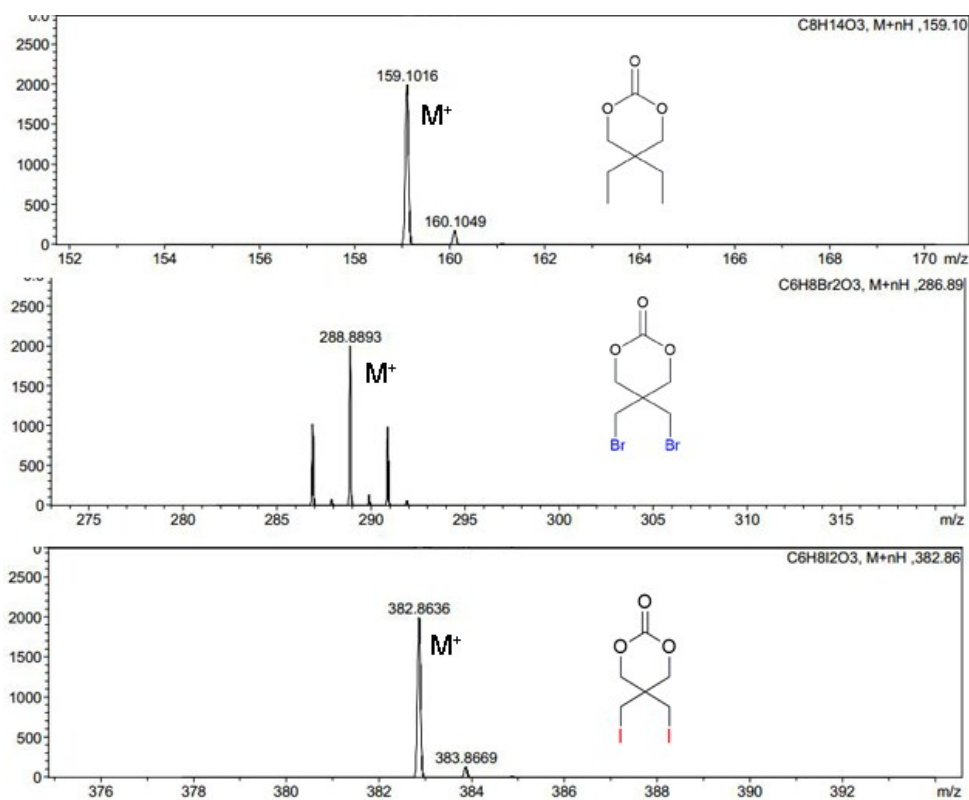


Fig. S5. High-resolution mass spectra of the resultant monomers.

Moreover, a peak at 623 eV pertaining to iodine element was detected in ITMC by XPS measurement (Fig. S6), indicating that the correct chemical composition of the ITMC monomer.

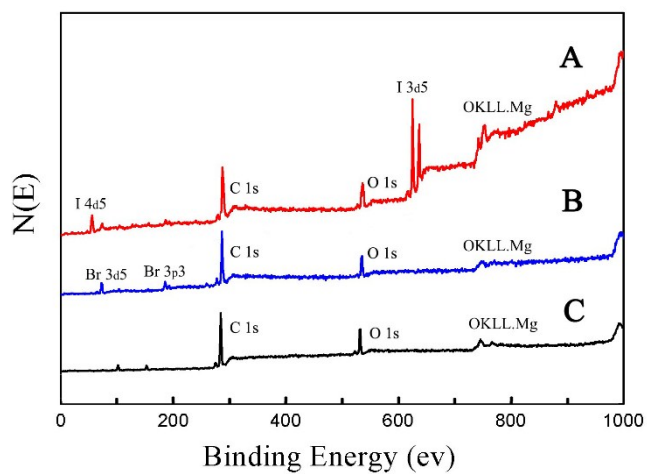


Fig. S6. XPS spectra of ITMC (A), BTMC (B) and ETMC (C).

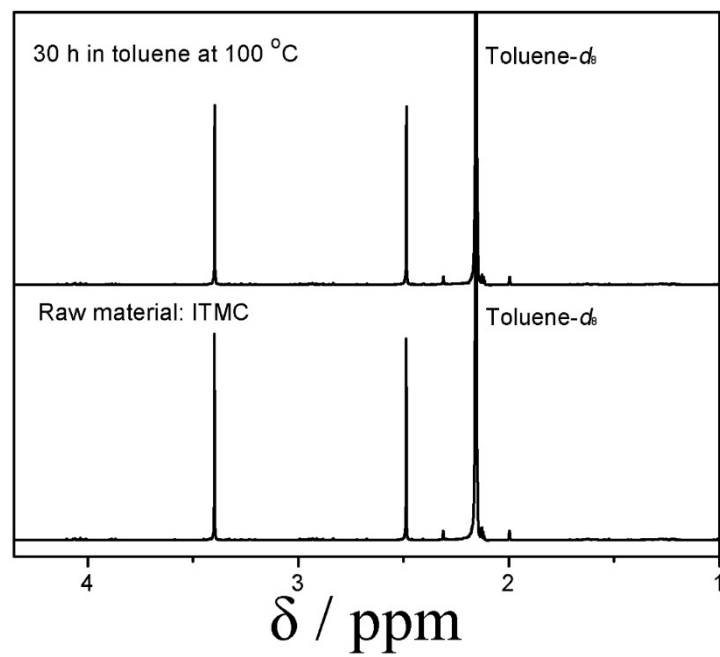


Fig. S7. ¹H NMR spectra of ITMC in toluene-*d*₈ before and at 100 °C for 30 h.

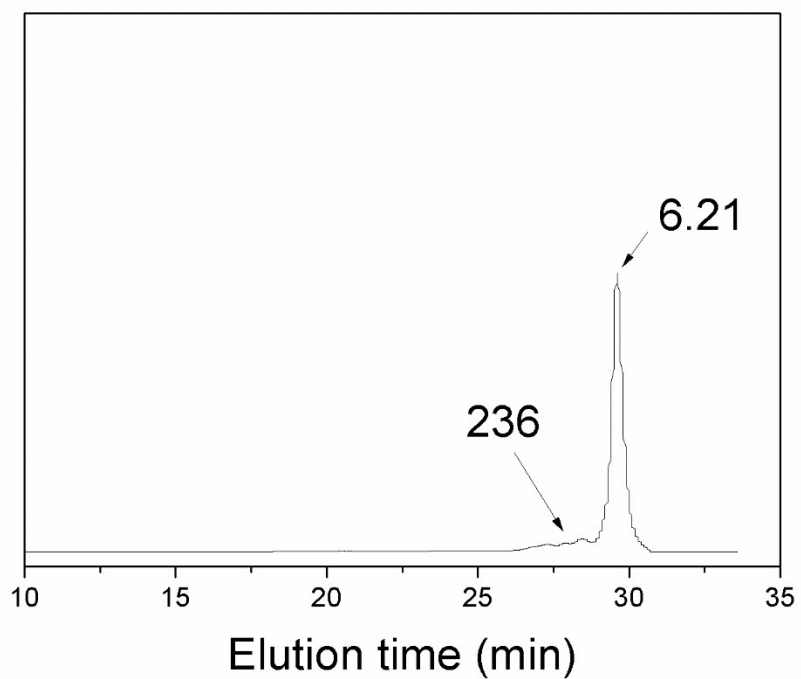


Fig. S8. GPC trace of the product after the polymerization of ITMC using 3-methyl-1-butanol as the initiator and stannous octoate as the catalyst.

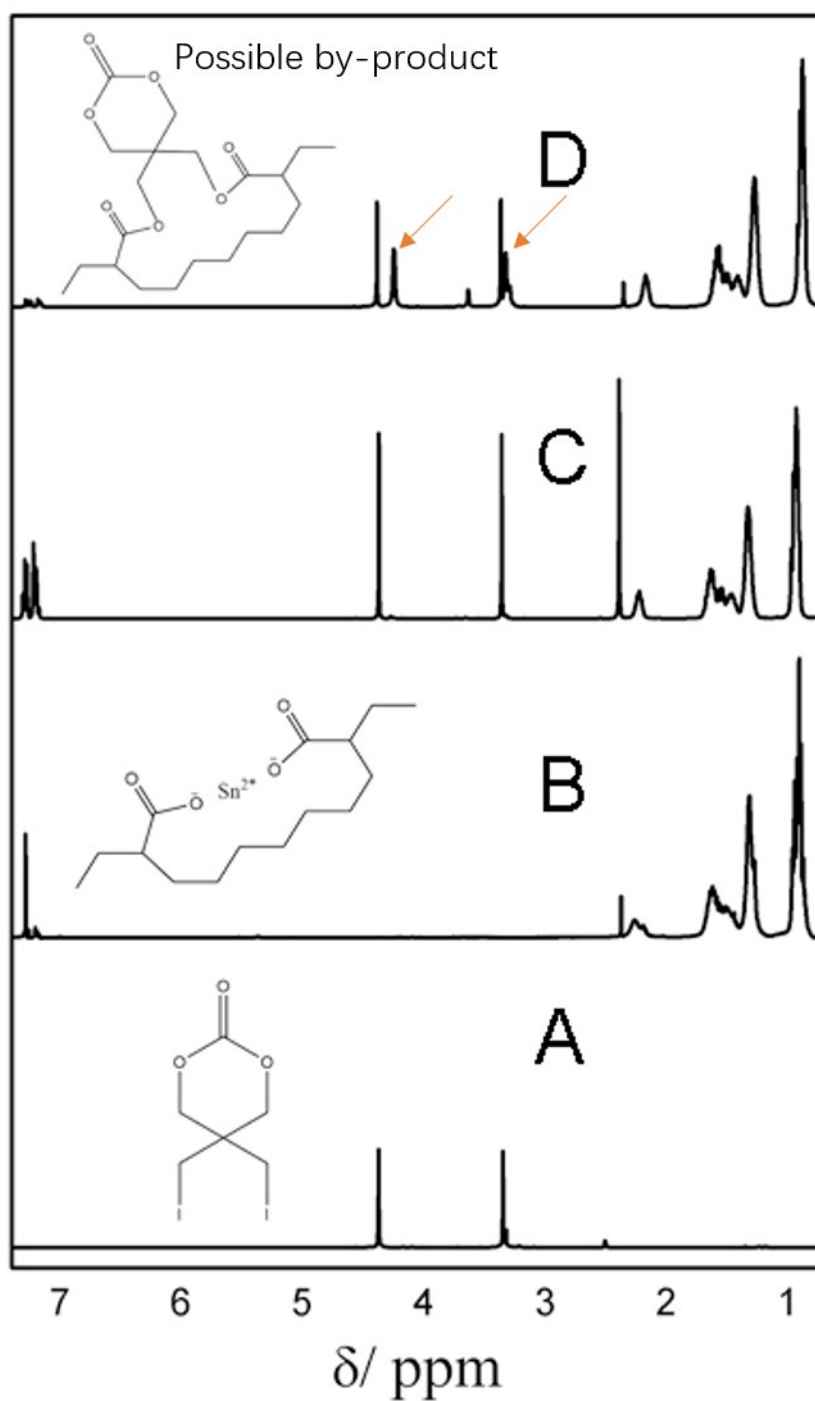
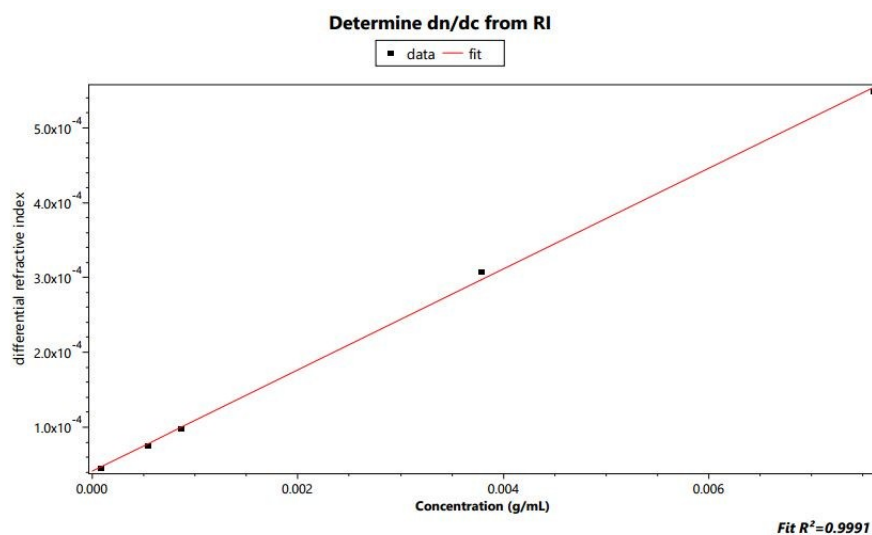


Fig. S9. ^1H NMR spectra: A) ITMC (100 °C); B) stannous octoate in toluene (100 °C); C) ITMC and stannous octoate in toluene (room temperature); D) ITMC and stannous octoate in toluene (100 °C).



Sample	M_n^a	M_w^b	M_w^c	dn/dc ^c
P1	6100	4200	5900	0.0674

a: M_n calculated from ¹H NMR.

b: M_w measured *via* GPC in THF using PS standards.

c: M_w and dn/dc measured *via* GPC-MALS-VIS

Fig. S10. dn/dc result of P1 measured by a refractive index detector in THF and its MW obtained from ¹HNMR, GPC and GPC-MALS-VIS.

Table S1 Polymerization kinetics of copolymer **P21**

Time (h)	$M_{n,NMR}^a$ (g mol ⁻¹)	$M_{n,GPC}^b$ (g mol ⁻¹)	\bar{D}_M^b	f_{ITMC}^a	In polymer ^a
1	9350	1900	1.16	57%	PCL ₁₅ -PITMC ₂₀
2	9920	2100	1.20	50%	PCL ₂₀ -PITMC ₂₀
3	8470	2200	1.21	38%	PCL ₂₄ -PITMC ₁₅
4	8690	3300	1.16	36%	PCL ₂₆ -PITMC ₁₅
5	9530	3300	1.20	35%	PCL ₃₀ -PITMC ₁₆
7	10220	3000	1.23	30%	PCL ₃₆ -PITMC ₁₆
9	10520	4000	1.22	26%	PCL ₄₂ -PITMC ₁₅
10	10970	3900	1.23	25%	PCL ₄₆ -PITMC ₁₅
13	15620	5300	1.30	22%	PCL ₇₀ -PITMC ₂₀
16	9830	4000	1.23	21%	PCL ₄₆ -PITMC ₁₂
17	10820	4800	1.21	22%	PCL ₄₈ -PITMC ₁₄
20	10820	5000	1.21	22%	PCL ₄₈ -PITMC ₁₄
24	10820	4200	1.21	22%	PCL ₄₈ -PITMC ₁₄
25	10930	3300	1.30	22%	PCL ₄₈ -PITMC ₁₄

The mole ratio of monomer to initiator is 50.

a: M_n , f_{ITMC} and copolymer composition calculated from ¹H NMR.

b: M_n and \bar{D}_M measured *via* GPC.

Table S2 Polymerization kinetics of copolymer **P25**

Time (h)	$M_{n,NMR}^a$ (g mol ⁻¹)	$M_{n,GPC}^b$ (g mol ⁻¹)	D_M^b	f_{ITMC}^a	In polymer ^a
0.5	3400	1700	1.15	12.5%	PITMC ₃ -PTMC ₁₁ -PCL ₁₀
1	7200	3300	1.14	11.5%	PITMC ₆ -PTMC ₂₈ -PCL ₁₈
2	7406	3500	1.26	13.5%	PITMC ₈ -PTMC ₂₇ -PCL ₁₄
3	7216	3700	1.31	14.0%	PITMC ₇ -PTMC ₃₀ -PCL ₁₃
4	7216	4100	1.28	14.0%	PITMC ₇ -PTMC ₃₀ -PCL ₁₃
5	7216	4100	1.25	14.0%	PITMC ₇ -PTMC ₃₀ -PCL ₁₃
6	7394	4100	1.26	16.3%	PITMC ₈ -PTMC ₂₈ -PCL ₁₃
13	8412	3900	1.31	16.0%	PITMC ₉ -PTMC ₃₂ -PCL ₁₅
16	14344	4200	1.22	17.0%	PITMC ₁₆ -PTMC ₅₅ -PCL ₂₃
20	9304	3600	1.40	16.1%	PITMC ₁₀ -PTMC ₃₇ -PCL ₁₅
25	9610	3200	1.34	15.4%	PITMC ₁₀ -PTMC ₄₀ -PCL ₁₅
27	9646	3500	1.27	15.4%	PITMC ₁₀ -PTMC ₃₇ -PCL ₁₈

The mole ratio of monomer to initiator is 50.

a: M_n , f_{ITMC} and copolymer composition calculated from ¹H NMR.

b: M_n and D_M measured *via* GPC.

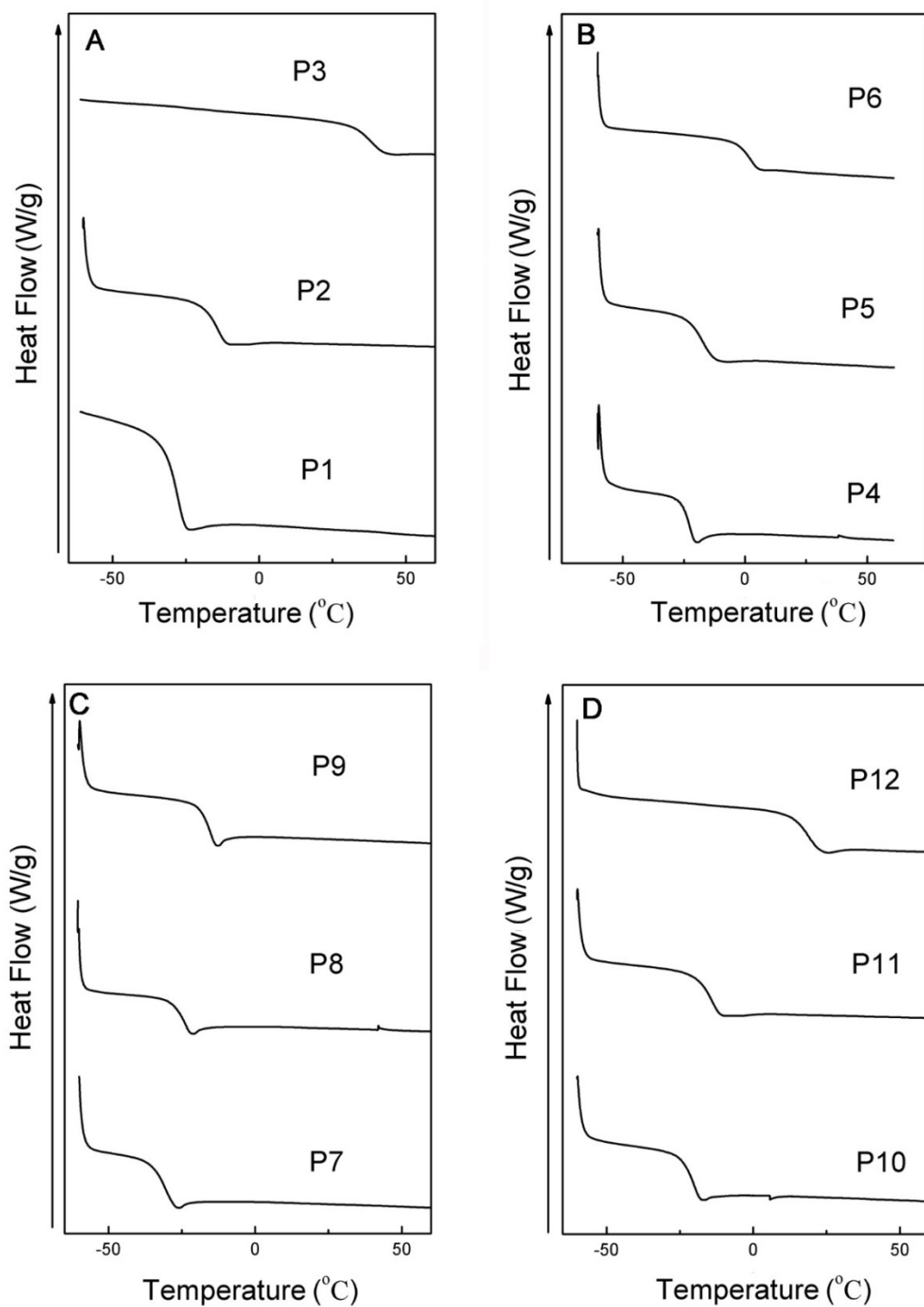


Fig. S11. DSC curves of copolymers **P1-P12** with varied mole ratios of monomers (A: P(TMC-*co*-ITMC) (30 h); B: P(TMC-*co*-BTMC); C: P(TMC-*co*-ETMC); D: P(TMC-*co*-PITMC) (16 h)).

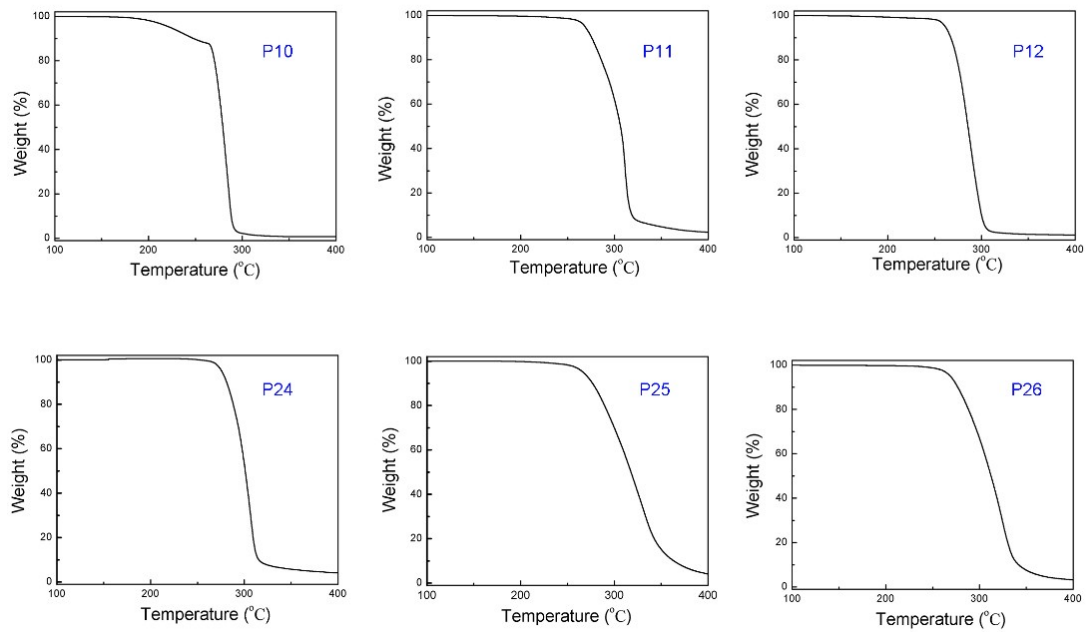


Fig. S12. TGA thermograms of some representative samples.

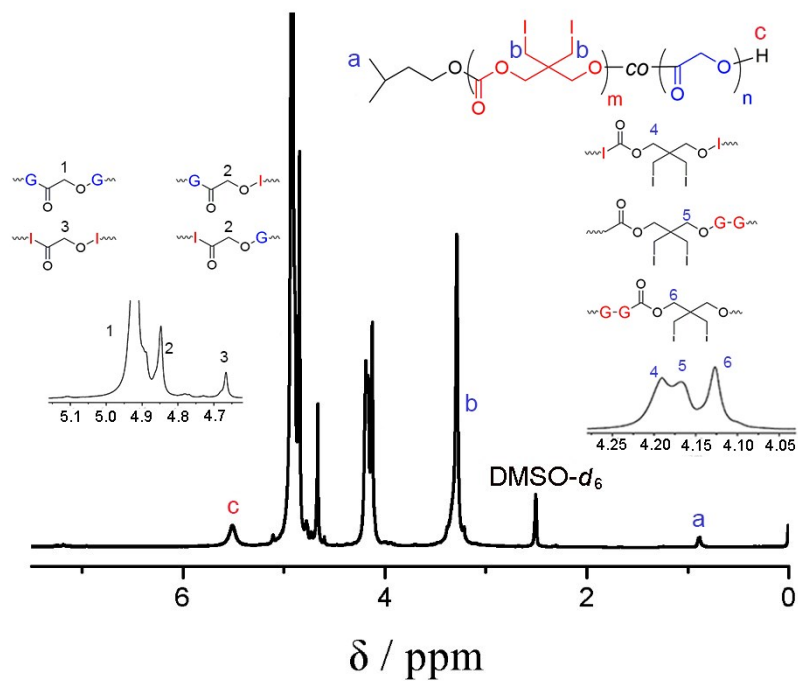


Fig. S13. ^1H NMR spectrum of the copolymer **P19** in $\text{DMSO-}d_6$. The peaks, as shown in the magnified local spectra, were assigned on basis of references.¹⁻³

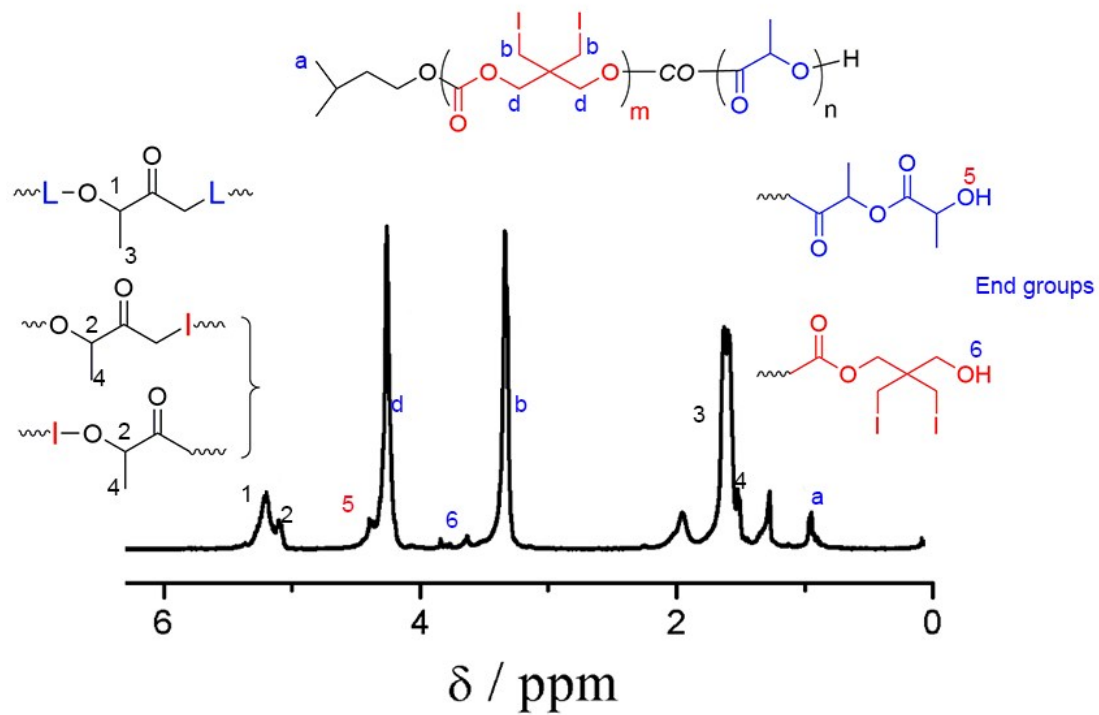


Fig. S14. ^1H NMR spectrum of the copolymer **P20** in CDCl_3 . The peaks, as shown in the magnified local spectra, were assigned on basis of reference.⁴

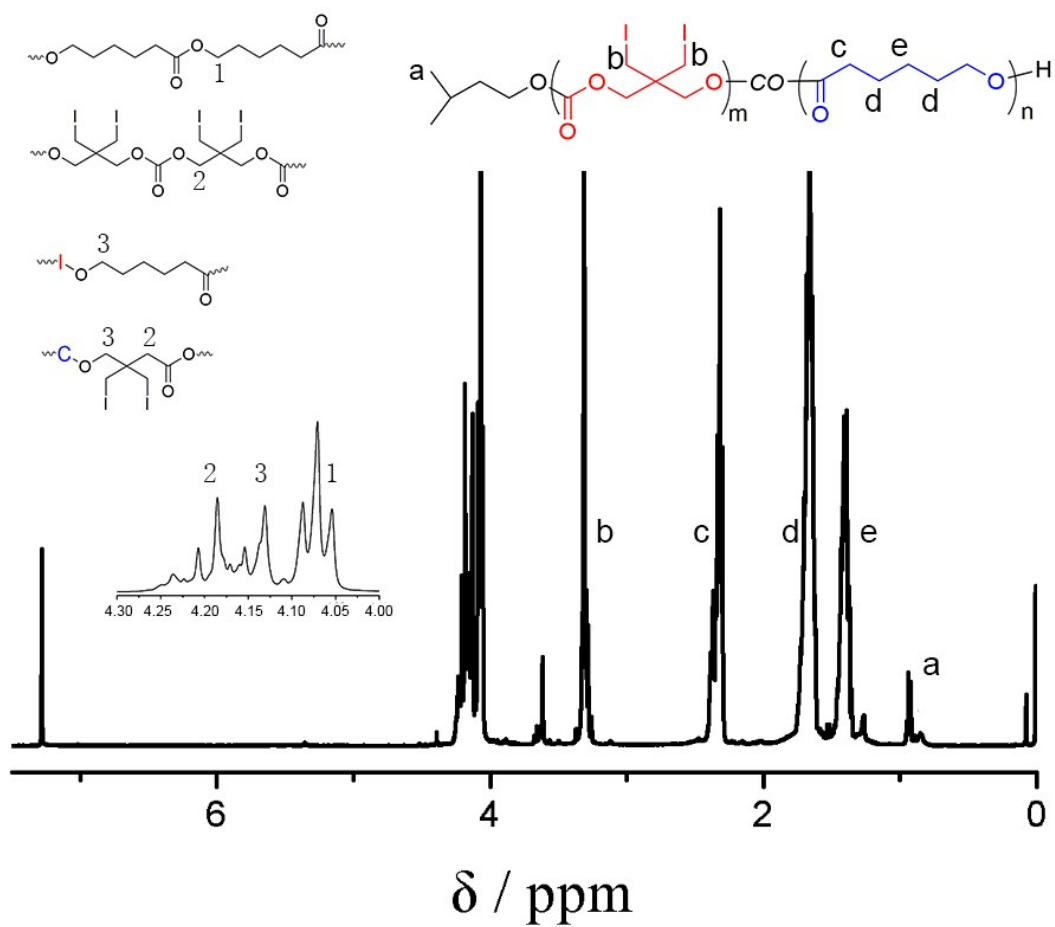


Fig. S15. ^1H NMR spectrum of the copolymer **P21** in CDCl_3 . The peaks, as shown in the magnified local spectra, were assigned on basis of references.^{5,6}

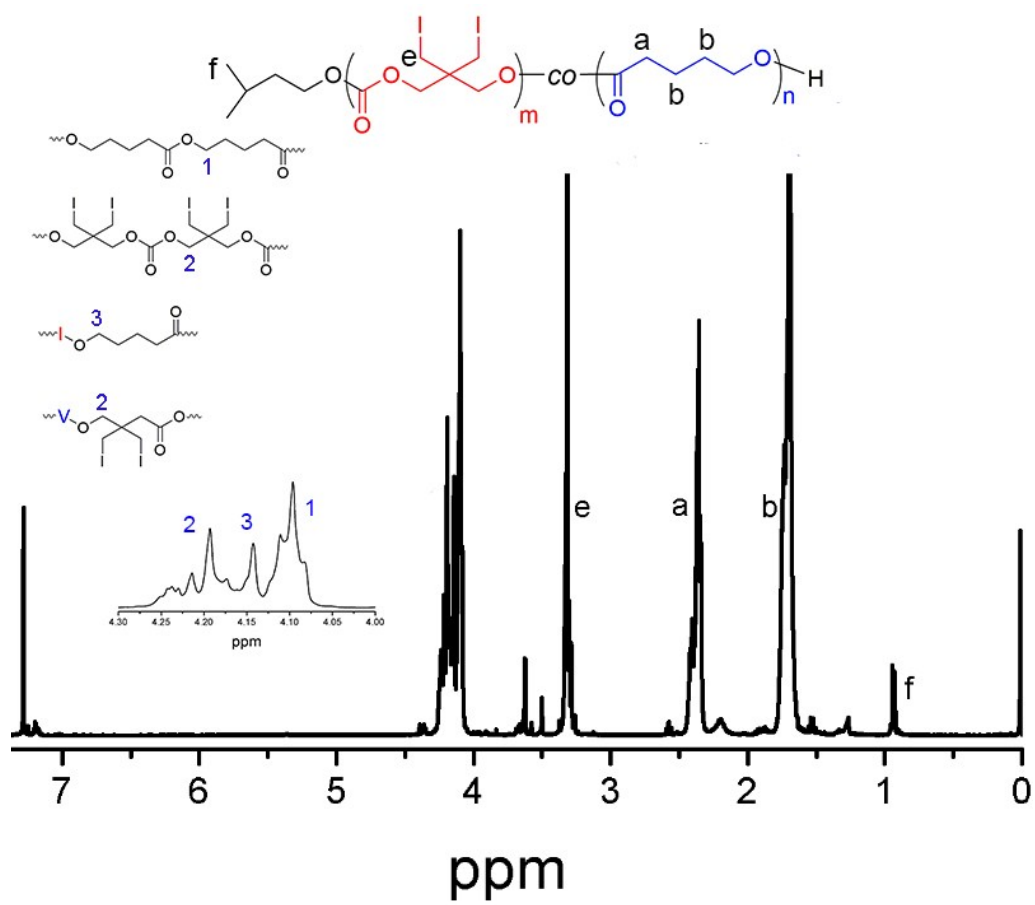


Fig. S16. ^1H NMR spectrum of the copolymer **P22** in CDCl_3 .

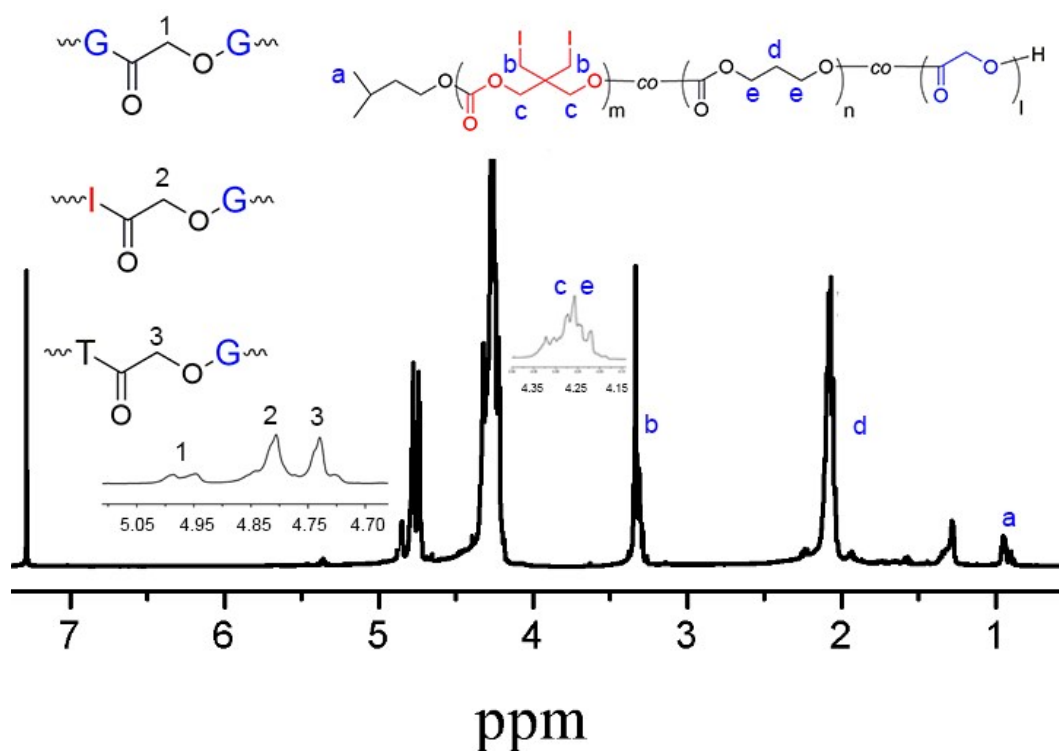


Fig. S17. ^1H NMR spectrum of the copolymer **P23** in CDCl_3 . The peaks, as shown in the magnified local spectra, were assigned on basis of references.^{2, 3, 7}

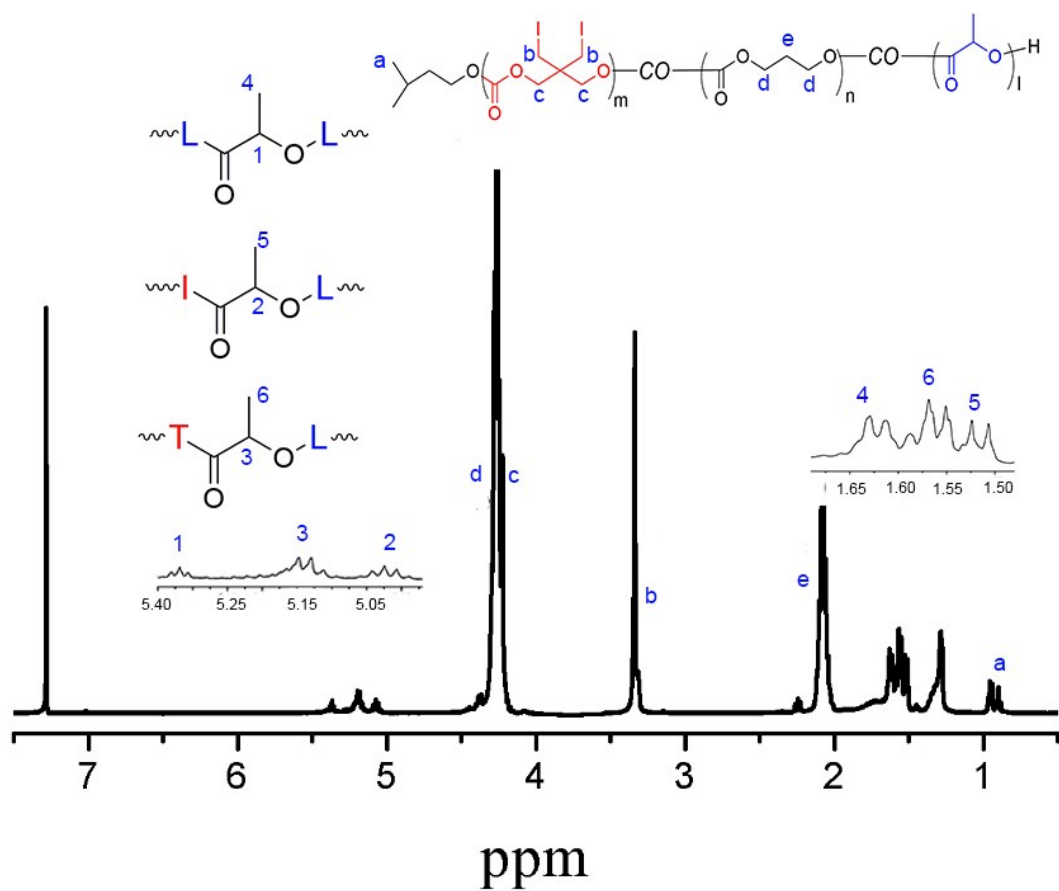


Fig. S18. ^1H NMR spectrum of the copolymer **P24** in CDCl_3 . The peaks, as shown in the magnified local spectra, were assigned on basis of reference.⁴

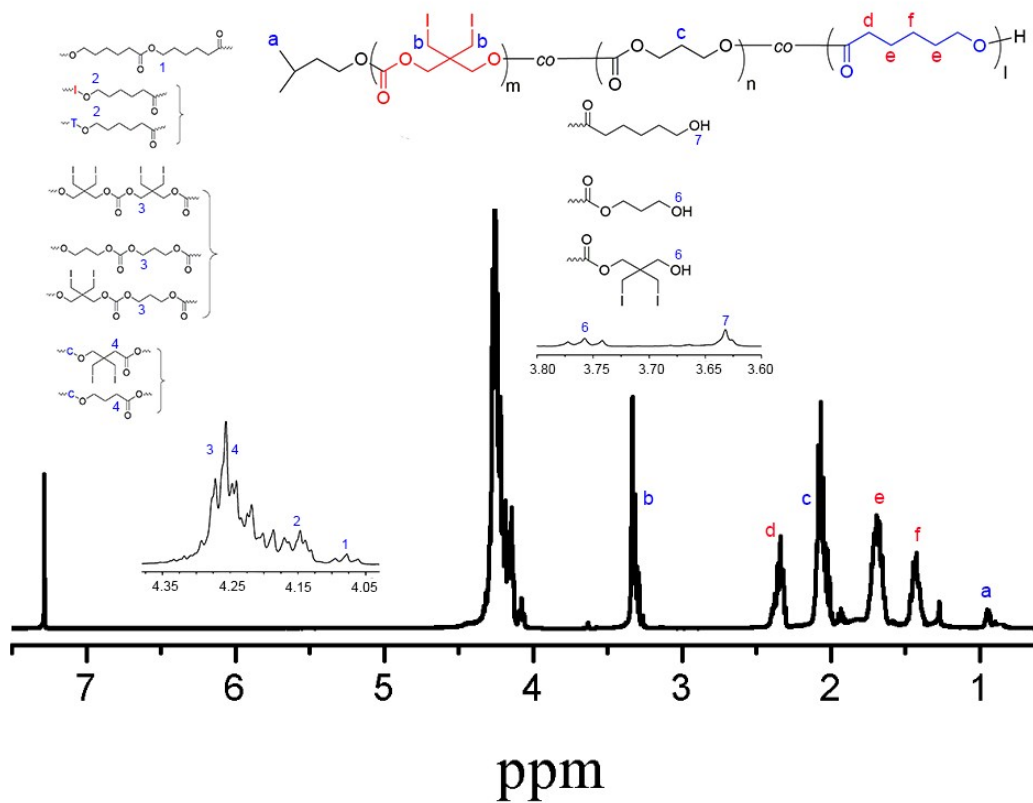


Fig. S19. ^1H NMR spectrum of the copolymer **P25** in CDCl_3 . The peaks, as shown in the magnified local spectra, were assigned on basis of references.^{5, 6}

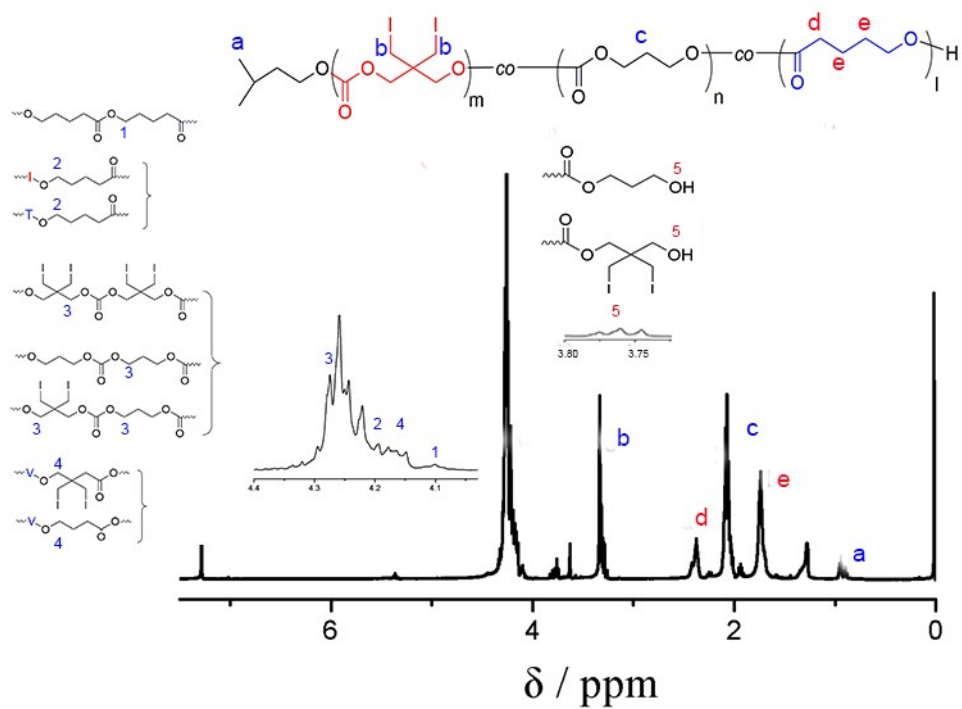


Fig. S20. ^1H NMR spectrum of the copolymer **P26** in CDCl_3 .

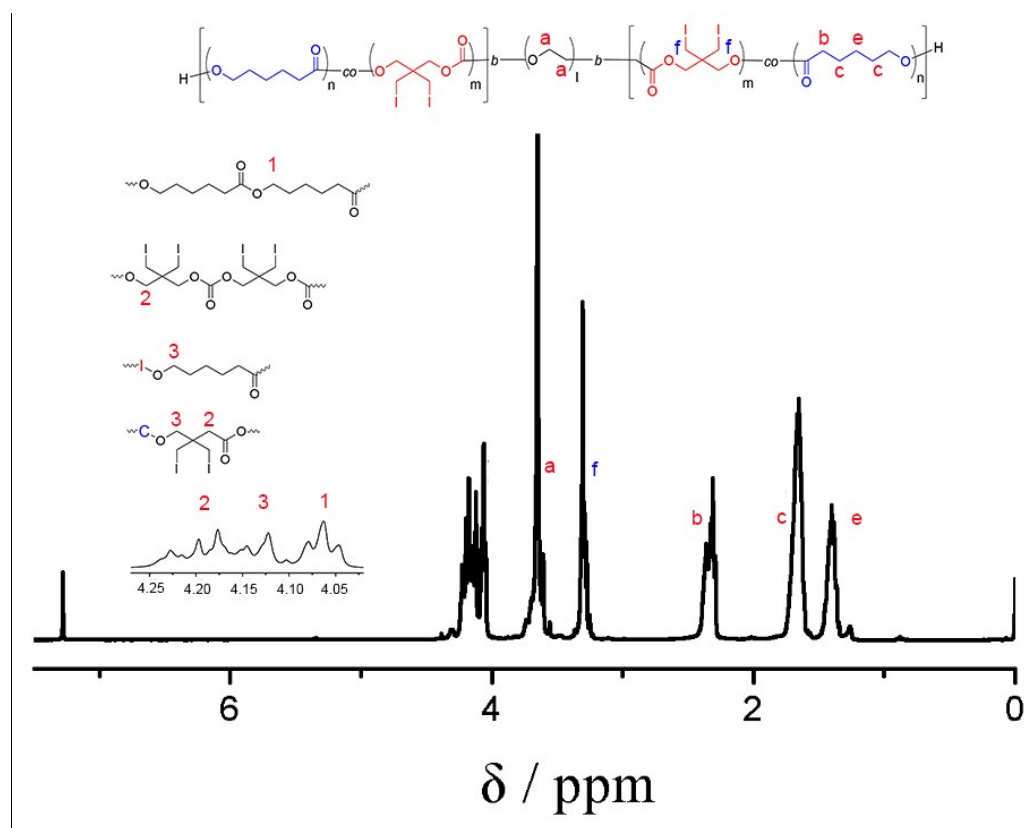


Fig. S21. ^1H NMR spectrum of the copolymer **P27** in CDCl_3 . The peaks, as shown in the magnified local spectra, were assigned on basis of references.^{5,6}

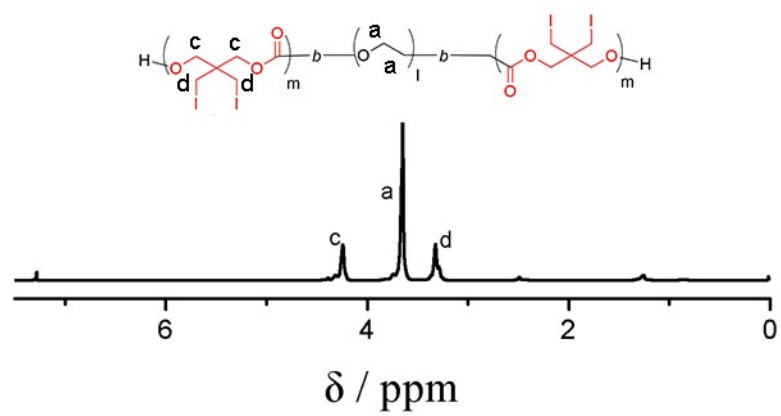


Fig. S22. ^1H NMR spectrum of the copolymer **P28** in CDCl_3 .

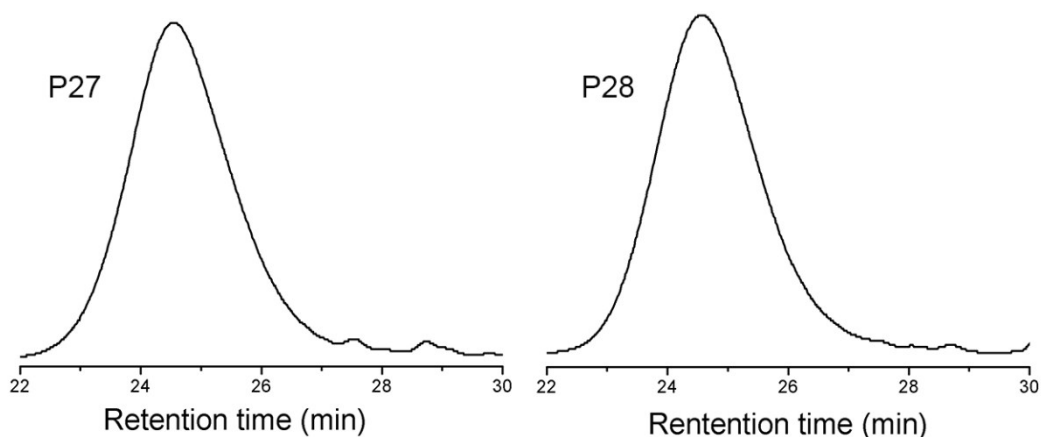


Fig. S23. GPC traces of P27 and P28.

Notes and references

1. E. Díaz-Celorio, L. Franco, A. Rodríguez-Galán and J. Puiggali, *Eur Polym J*, 2012, **48**, 60-73.
2. R. Zurita, L. Franco, J. Puiggali and A. Rodríguez-Galán, *Polym Degrad Stabil*, 2007, **92**, 975-985.
3. E. Díaz-Celorio, L. Franco, A. Rodríguez-Galán and J. Puiggali, *Polym Degrad Stabil*, 2013, **98**, 133-143.
4. S. Agarwal, M. Puchner, A. Greiner and J. H. Wendorff, *Polym Int*, 2005, **54**, 1422-1428.
5. Q. Song, Y. Xia, S. Hu, J. Zhao and G. Zhang, *Polymer*, 2016, **102**, 248-255.
6. J. Ling, W. Zhu and Z. Shen, *Macromolecules*, 2004, **37**, 758-763.
7. S. C. Lee, K. J. Kim, S. W. Kang and C. Kim, *Polymer*, 2005, **46**, 7953-7960.